Edelweiss Applied Science and Technology
ISSN: 2576-8484
Vol. 8, No. 6, 9411-9424
2024
Publisher: Learning Gate
DOI: 10.55214/25768484.v8i6.4018

Pore water pressure of sandy soil improved with steel slag under the influence seismic load

Hassan Ali Ahmed[1*], Jawdat K. Abbas[2]
[1,2]College of Engineering, Tikrit University, Tikrit, Iraq; mr.hassanali@tu.edu.iq (H.A.A.) dr.jawdatkhadim@tu.edu.iq (J.K.A.).

Abstract: In this study, we examined the change in pore water pressure and the liquefaction phenomenon on sandy soils improved using steel slag, which is one of the industrial wastes of iron and steel factories, with a mixing ratio of (3,6,9,12,15) % using a shaking table under the influence of the Halabja earthquake, which is active in the seismic zone located in northeastern Iraq, the foundation that was used in the examination is a circular foundation with dimensions of (100) mm diameter. Pore water pressure sensors, number A, were placed inside the soil, where the first was at a distance of 5cm from the bottom of the foundation and the second was at a distance of 25cm from the bottom of the foundation. Based on the previous findings, the pore water pressure is higher at a depth of 5 cm than at 25 cm, adding steel slag to the sandy soil led to a reduction in the pore water pressure over the two distances that were measured from the bottom of the foundation, where the higher the percentage of steel slag after 6, the lower the value of the pore water pressure, When steel slag is added at depths of 5 and 25 cm, the Halabjah earthquake exhibits non-linear, overlapping behavior that intensifies as steel slag is added.

Keywords: *Circular footing, Halabjah earthquakes, Pore water pressure, Sandy soil, Steel slag.*

1. Introduction

The methods created to lessen liquefaction fall into four groups: partially soaking the soil, treating liquefiable soil with nanomaterials and synthetic fibers, employing recycled materials for backfills, and enhancing the soil with grouting materials like microfine cement or bio-cementation. The problems of increased effort, high expense, complex operation, potential damage to nearby structures, and environmental pollution associated with typical cement operations can be addressed using microfine cement, nanomaterials, or biological materials. However, controlling the penetration area, getting uniform penetration, guaranteeing the required gel length, and maximizing gelation conditions are challenges for engineering practice. To accomplish constant infiltration across a large region or structure near existing buildings, more research is required to find a more straightforward and effective technique. The partial saturation technique in laboratory investigations can provide significant data Bao et al. (2019).

Nevertheless, further investigation and examination are required to comprehend the process and its long-lasting nature comprehensively. Using recycled materials for liquefaction mitigation is a highly effective method that conserves resources and is environmentally friendly. However, further efforts are required to incorporate it into engineering procedures. Overall, it has been shown that these newly discovered strategies for mitigating liquefaction are effective to different extents Bao et al. (2019).

Arulandan and Sybico Jr. (1992) found that sand's permeability increases beyond the initial site of liquefaction, which led them to conclude that this rise in permeability is the cause of large settlement after liquefaction.

Saglam (2011) The surplus pore water pressure ratio increases rapidly at the initial stages of axial strain, particularly reaching roughly 5-6% DA for tests with stress reversals and 2-4% SA for tests without stress reversals. The gradient of the graph indicates the relationship between the ratio of excess

* Correspondence: mr.hassanali@tu.edu.iq

pore water pressure and axial strain, which starts to decrease beyond certain levels of axial strain. The extra pore pressure ratio is predominantly found to range from 40% to 60% at the flexure point. The excess pore water pressure ratio range is far below the threshold for initiating liquefaction.

Sun et al. (2011) carried out the subway station's structure underwent a shaking table test in the layer of liquefied sand. The findings demonstrated that liquefaction dampened the subterranean structure and considerably raised the structure.

Ecemis (2013) looked at the accuracy and consistency of measurements made with a shaking table and laminar box in addition to the outcomes.

Mominul et al. (2013) discovered that when shear strain rose, the damping ratio increased and the shear modulus decreased. The most intriguing discovery is that sand's liquefaction resistance decreases with increasing silt content, up to 30%. The liquefaction resistance of the soil showed negligible variation with silt concentration above 30%.

Akinwumi (2014) demonstrated that, in the absence of unfavorable swell behavior, crushed steel slag might be employed to improve the lateritic soil's plasticity, uncured strength, and drainage properties. Only when 8% steel slag was added to the soil did the uncured strength of the soil improve. When 8% steel slag was added to the soil, its unconfined compressive strength improved by 66.7 kN/m2 and its unsoaked CBR increased by 40%.

Hong et al. (2015) The sand-tire mixture was determined to be significantly more compressible than pure sand while having generally more significant peak friction angles. The liquefaction resistance of pure sand is more excellent than that of the sand-tire mixture prepared using the air-drying method; nevertheless, it is lower than that prepared using the oven-drying method. Moreover, the sand-tire combination exhibits an enhanced liquefaction resistance as the tire chips' size increases. This suggests that the size and condition of the tire chips substantially impact the liquefaction behavior of the tire chips-sand mixture.

Chen et al. (2015) conducted several shaking table experiments on the Nanjing rail transit structure, including soft soil and liquefiable soil model foundations, frame and three-arch column model station structures, and other material models. The main subjects of the study were the deformation and seismic impact on soil, namely on concrete and gypsum structures. It also looked at how failure and deformation affect the subterranean subway construction.

Otsubo et al. (2016) The utilization of recycled waste materials such as crushed glass, crushed concrete, a combination of tire chips and sand, and cement-mixed liquefaction ejecta has effectively addressed the issue of liquefaction-induced floating of buried pipes. Additionally, well-compacted backfills, due to their high unit weight, have the tendency to settle when the surrounding subsoil liquefies. To prevent subsidence, it is necessary to modify the unit weight of the backfill to correspond with the liquefiable subsoil in the surrounding area.

Ye and Hu (2018) Concluded that settlement is higher in looser sand, that permeability influences the development of pore pressure, and that permeability declines with density.

Ye et al. (2018) examined the mesoscopic structure of sand and explained that the sand particle's horizontal long-axis direction changing to a vertical one during the virgin condition was the only reason for the decrease in re-liquefaction resistance observed in the second event. Density was found to be a major component determining the re-liquefaction phenomenon after the second liquefaction, as this vertical direction continued afterward. In this way, it is believed that in the case of another earthquake, the site, having already liquefied, may liquefy once more.

Abed, N., and Abbas, J. K. (2020) describe gypsum soil behavior and features. Based on gypsum weight, the soil received 5%, 7.5%, 10%, 12.5%, and 15% iron fillings. Chemical, physical, and engineering testing followed, and adding 0% to 5% additives improved soil engineering. The intervention reduced soil collapse from 5.08 to 1.16 and increased cohesiveness from 29.34 to 50.02 KN/m3. In addition, the soil's internal friction angle increased from 33.19° to 43°.

Hazarika et al. (2020) Tire chips have proven to be a highly effective material for avoiding liquefaction. Nevertheless, the utilization of these materials directly may lead to undesirable settlement of buildings supported by them, owing to their compressible characteristics. Using gravel-mixed tire chips as the horizontal inclusion will increase the shear stiffness in the reinforced layer. Therefore, the

Edelweiss Applied Science and Technology
ISSN: 2576-8484
Vol. 8, No. 6: 9411-9424, 2024
DOI: 10.55214/25768484.v8i6.4018

settlement will be reduced, the horizontal diversity will have a thickness of 10 cm (equivalent to 2 m in the prototype), and the gravel proportion will be 50%. The technique used to mitigate liquefaction provides the most effective results, as it limits the increase in surplus pore water pressure. As a result, the settlement of the structure caused by earthquakes is finally reduced.

Nepal and Chen (2021) found that the depth of the sand layer influences the re-liquefaction phenomenon and that shallower sand layers are more prone to multiple liquefaction than deeper sand layers because, when input motion stops, the sand particles sink towards the depth and upper particles fall on it, making the top portion relatively loose. Within a zone, a key liquefaction void ratio allows us to predict whether re-liquefaction will occur during the next earthquake.

Lindh and Lemenkova (2022) Compared to other mixes, the combination of slag and energy fly ash has the least effect on strength increase. A factor test that combined blended binders of different mixtures allowed researchers to examine the conditions under which two factors interact during the soil stabilization process, determining whether or not the final product's quality will be approved. For example, if soil treatment is performed in a sub-area with a high water and contaminant content.

To prevent foundation settlement damage, Hasen, N. A., and Abbas, J. K. (2024) studied sandy soil reinforcement following the three earthquakes (Halabjah, Bolunun, and Ali Al-Gharbi). Five-layer geogrid shaking table studies investigated 70%-density sand samples with and without reinforcement. Dynamic force settles. Thus, the 100 * 100 * 30 mm plastic foundation was chosen. Static load: 5.294 kN/m^2. Seismic acceleration settles sandy soil foundations. More geogrid layers lower base settlement faster and reduce seismic acceleration. Settlement and start times are always the same. Wet soil settles twice as fast.

2. Material and Method

2.1. Materials

2.1.1. Characteristics of Sandy Soil

The sand used in the trials was from a nearby river, which is widely accessible and typically used for most construction projects. It was transported from the Tuz region in the heart of Iraq, which is situated in the Salah-Aldeen Governorate 80 kilometers east of Tikrit. A suitable amount was sieved via sieve No. 4 prior to the testing commencing. Through the use of engineering experiments, including direct shear, and classification tests, the properties of the soil were ascertained.

2.1.2. Properties of the Steel Slag

The source of this trash was the steel industry located in Sulaymaniyah Governorate's Bazian area. The iron Arc process yields this residue as a byproduct. To check the percentage of silica and lime, a chemical test was run. After that, the slag was broken up using a jaw crusher and sieved to a 250-micron size (No. 60). Using a hand shovel, the steel slag and sand were combined until the material was homogenized. The results of Tikrit University's College of Engineering's Department of Chemical Engineering laboratory tests are displayed in Table 1. Figure 1 shows the final form of steel slag after grinding and passes through sieve No.60.

Edelweiss Applied Science and Technology
ISSN: 2576-8484
Vol. 8, No. 6: 9411-9424, 2024
DOI: 10.55214/25768484.v8i6.4018

Figure 1.
Shows the steel slag.

Table 1.
The chemical composition of iron slag used in the present study.

Chemical components	Percentages (%)
Fe_2O_3	42.01
SiO_2	14.27
Al_2O_3	2.81
MgO	2.08
CaO	32.96
Other	5.87

2.2. Test Process

2.2.1. Mechanical Components of a Shaking Table

All research and design development for the shaking table, which supports the cart's 80 by 80 by 8 cm base with a 60 by 120 by 10 cm steel framework screwed to the ground, is complete. Wheels coupled to sliding steel tubes move the base of the cart. Rubber sheets 10 mm thick supported the exterior frame. Keeps the rubber pad flush with the floor and the gadget from vibrating. Figure 2 shows how a 40-mm ball screw shaft with a 750-mm length, 620-mm travel, and 40-mm diameter converts the motor's rotational motion into linear displacement in the shaking table. Two ball screw nut brackets were added to the shaking table frame. One bracket supported the drive rod, the other was fastened to the frame of the rocking table. fastens the ball screw, enabling movement of the frame.

Edelweiss Applied Science and Technology
ISSN: 2576-8484
Vol. 8, No. 6: 9411-9424, 2024
DOI: 10.55214/25768484.v8i6.4018

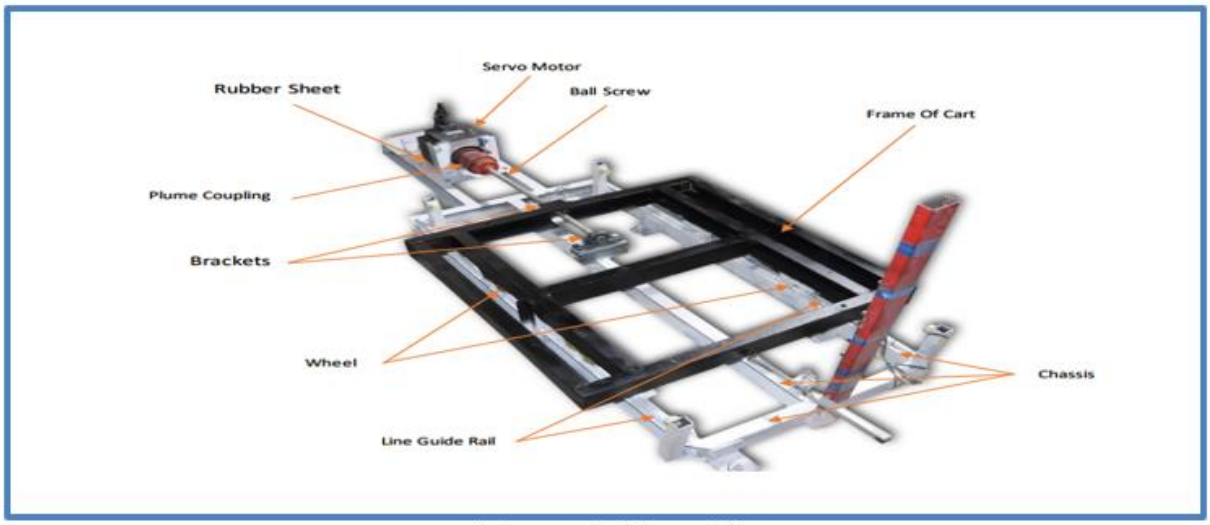

(a) Base shaking table.

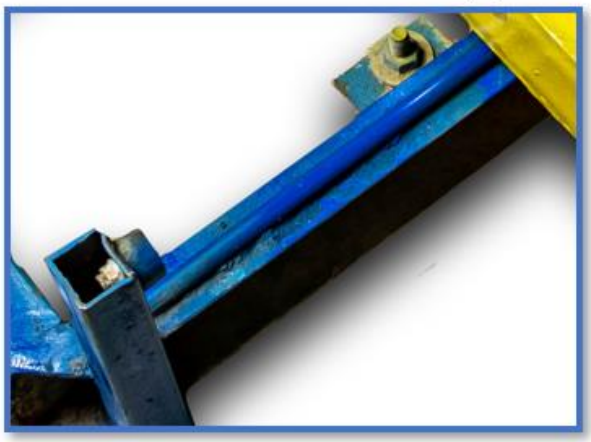

(b) Sliding steel tubes

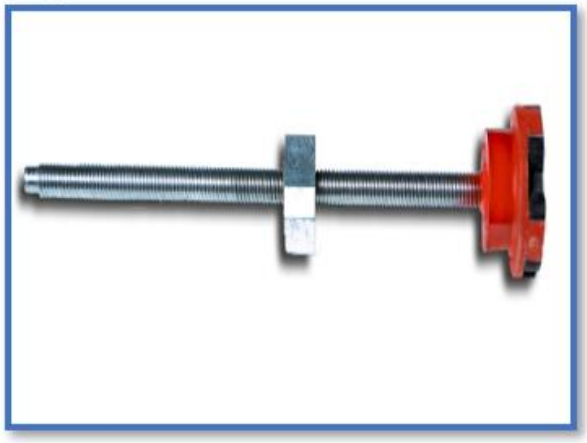

(c) Screw shaft.

Figure 2.
The mechanical parts of a shaking table.

2.2.2. Earthquake Simulator PC Software

The Earthquake Simulator software was developed using the graphical user interface code of LabVIEW 2020. The application manages shaking, shaking acceleration, data collection (DAQ), data logging, data analysis, and reporting. The LabVIEW program is necessary to program this system. A flexible tool called Data Logar incorporates input/output functionalities with real-time control for industrial applications. The system comprises a real-time controller, an architecture for adaptable input/output modules, and a programmable gate array (FPGA). This technology is well-suited for signal processing, high-speed control, specific hardware tasks, hardware algorithms, and signal processing due to its strong and durable nature and high performance.

Additionally, it offers unique triggering and timing capabilities. Figure 3 illustrates the components of the data logger, together with its input and output units. The chassis can accommodate eighteen input modules and two output modules. Each unit contains numerous channels specifically tailored to serve a particular purpose. The Earthquake Simulator consists of two primary phases:

Edelweiss Applied Science and Technology
ISSN: 2576-8484
Vol. 8, No. 6: 9411-9424, 2024
DOI: 10.55214/25768484.v8i6.4018

(a) Computer-controlled data logger

(b) Data logger component.

(c) Input and output devices.

Figure 3.
The data logger and components.

3. Result and Discussion

The previous seismic events resulted in the dissolution of the saturated sand, which caused extensive damage to multiple buildings, structures, and infrastructural components. Due to the disastrous nature of this kind of failure, liquefaction has been well-researched and documented, with a strong focus on comprehending the components that contribute to its occurrence.

When an earthquake occurs in a region with saturated sandy soil, the water pressure in the soil's pores increases rapidly and reaches a high level quickly. Drainage issues arise when the pressure rapidly rises to a high degree. As expeditiously as feasible, irrespective of the thickness of the existing stratum of porous sand. In the liquefaction stage, a significant reduction in shear strength is caused by an increase in pore water pressure. Subsequently, the liquid migrates from areas with elevated pressure to areas with reduced pressure. Pore water pressure rises towards lower-pressure regions to equilibrate the hydraulic pressure.

This phase is commonly known as the dissipation stage. The substance infiltrates the soil particles, which settle as a result of vibration, causing the particles to rearrange and restructure themselves, reestablishing contact, enhancing their strength, and filling the voids left by water dispersion. Following the period of shaking, the loose sand consolidates. Figure 4 depicts the occurrence of

Edelweiss Applied Science and Technology
ISSN: 2576-8484
Vol. 8, No. 6: 9411-9424, 2024
DOI: 10.55214/25768484.v8i6.4018

liquefaction in a solitary, loosely packed sandy layer. Conversely, figure 2 illustrates the influence of the earthquake on the pressure of pore water and the consequent liquefaction in the sandy soil.

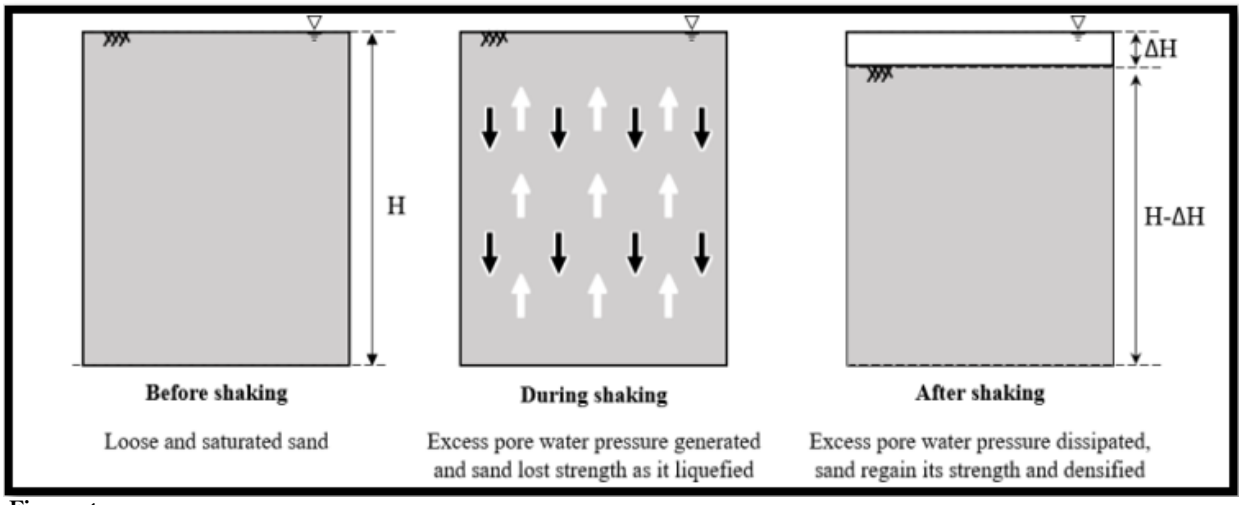

Figure 4.
Illustrates the liquefaction process. occurring within a solitary layer of loosely packed sand.

Table 2 and Figures 5 to 7 indicate that the unimproved sandy soil had the highest pore water pressure, as observed during the Halabjah earthquake. At a depth of 5 cm, it was found that the pore water pressure at the surface (referred to as (u1) pore water pressure) decreases gradually as the amount of steel slag material increases. The reduction rate varies, with the highest drop occurring when 6% steel slag is added. With each improvement scenario, Pore water pressure values drop until 15% of the steel slag is mixed in. The unimproved soil showed the maximum value of pore water pressure at a depth of 25 cm (u2). Furthermore, the rate at which the pore water pressure diminishes intensifies with the rise in steel slag content.

Additionally, it was noted that the drop's values are erratic and shifting, with the most significant decrease occurring at 6% steel slag in addition to the pore water pressure. Based on the prior, the pore water pressure is higher at a depth of 5 cm than at a depth of 25 cm. Similarly, the rate of decline changes and varies, although Table 2 suggests that the eventual erosion rate is higher at a depth of 5 cm based on those facts.

Moreover, the addition of steel slag had no effect on the time needed to reach the maximum pore water pressure, a consistent finding across all situations. As the steel slag content increased at depths of 5 and 25 cm, Figure 7 reveals a non-linear, overlapping, and growing pattern of pore water pressure in the Halabja earthquake, adding a layer of complexity to the process.

Edelweiss Applied Science and Technology
ISSN: 2576-8484
Vol. 8, No. 6: 9411-9424, 2024
DOI: 10.55214/25768484.v8i6.4018

Table 2.
The impact of the Halabjah earthquake on the Public Welfare Program (PWP).

Case of soil	The decrease in PWP at a 5 cm depth.	The percentage decrease in the PWP rate overall at a depth of 5 cm.	The decrease in PWP at a 25 cm depth.	The percentage decrease in the total PWP rate at a depth of 25 cm.
Unimproved soil	-	-	-	-
3% of steel slag	1.92%	1.92%	0.82%	0.82%
6% of steel slag	0.088%	2.008%	1.375%	2.195%
9% of steel slag	5.11%	7.118%	4.797%	6.985%
12% of steel slag	3.83%	10.94%	5.485%	12.47%
15% of steel slag	2.87%	13.818%	1.887%	14.357%

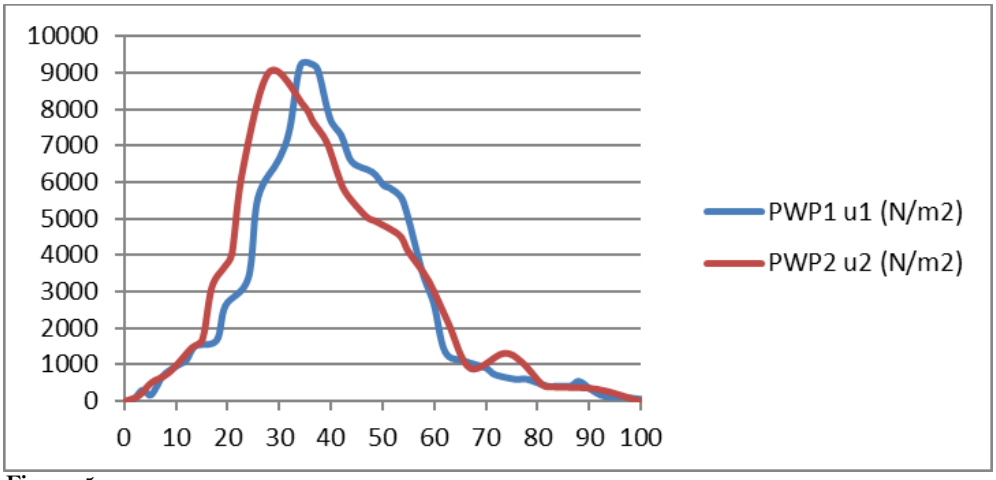

Figure 5.
PWP at Halabjah Earthquake of Unimproved Saturated Sandy Soil.

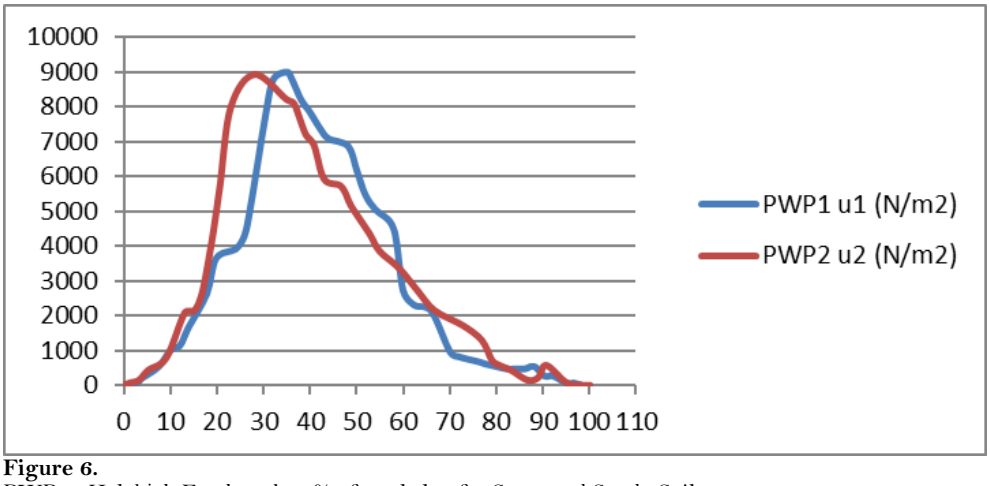

Figure 6.
PWP at Halabjah Earthquake 3% of steel slag for Saturated Sandy Soil.

Edelweiss Applied Science and Technology
ISSN: 2576-8484
Vol. 8, No. 6: 9411-9424, 2024
DOI: 10.55214/25768484.v8i6.4018

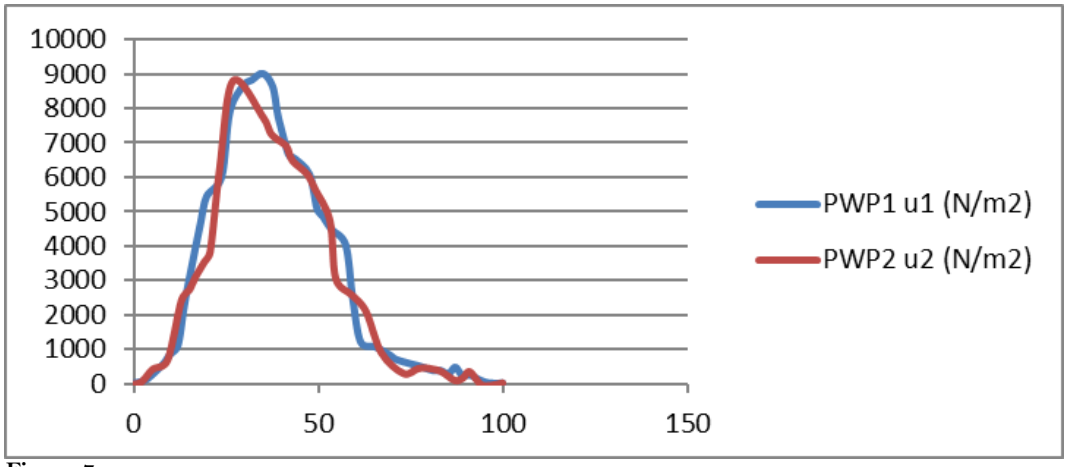

Figure 7.
PWP at Halabjah Earthquake 6% of steel slag for saturated sandy soil.

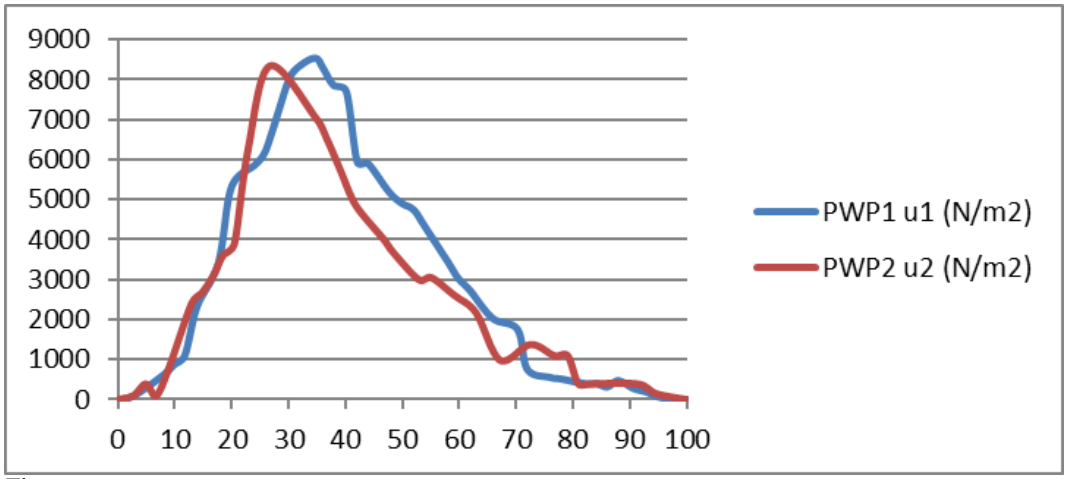

Figure 8.
PWP at Halabjah Earthquake 9% of steel slag for saturated sandy soil.

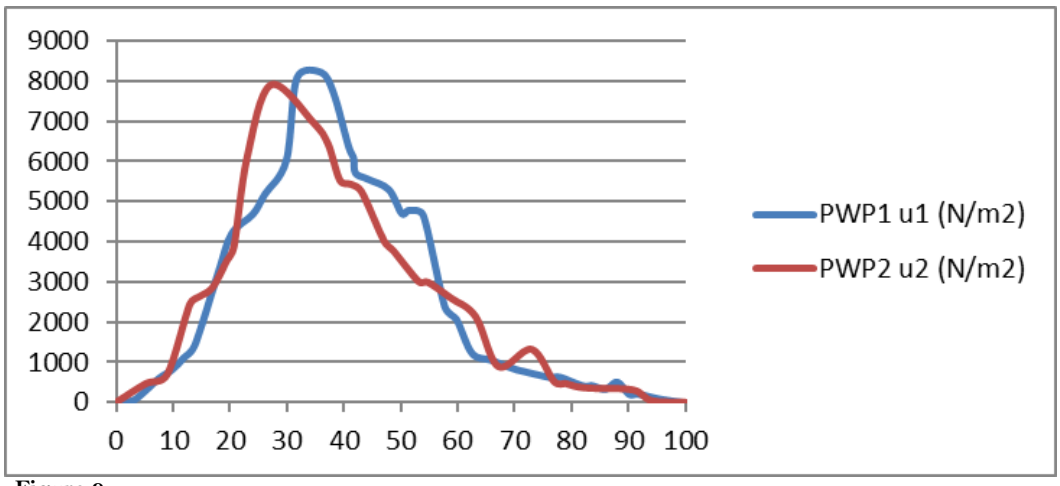

Figure 9.
PWP at Halabjah Earthquake 12% of steel slag for saturated sandy soil.

Edelweiss Applied Science and Technology
ISSN: 2576-8484
Vol. 8, No. 6: 9411-9424, 2024
DOI: 10.55214/25768484.v8i6.4018

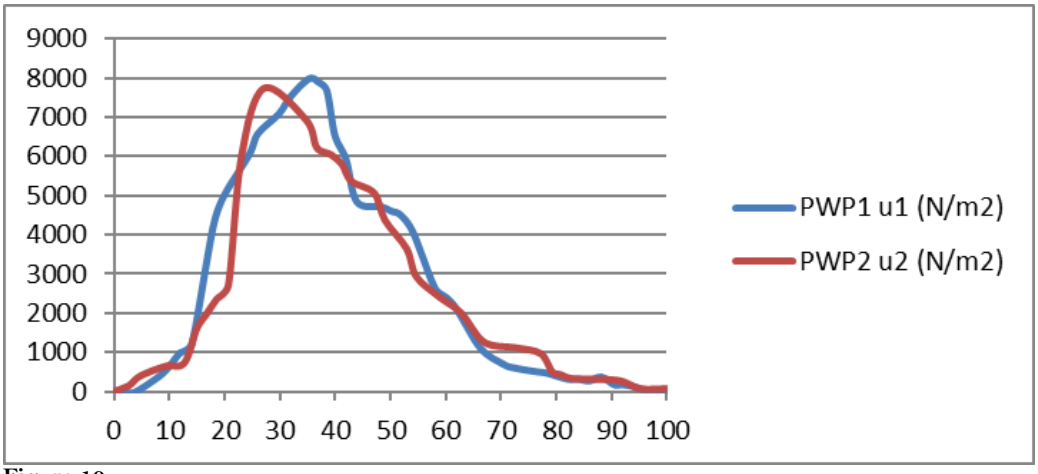

Figure 10.
PWP at Halabjah Earthquake 15% of steel slag for saturated sandy soil.

Based on the data presented in Table 3 and Figures 11 to 16, it is obvious that the Halabjah earthquake results in a gradual accumulation and increase in pore water pressure. This suggests that the sandy soil becomes more akin to a liquid as it loses its capacity to withstand pressure and maintain cohesiveness. This shift is explained by increased extra water pressure inside the sand grain pores. The earthquake's mechanical effect is responsible for this sudden rise, upsetting the equilibrium and cohesiveness between the soil particles and the water molecules in the gaps. Additionally, how the soil particles are arranged is important. Compacted soil has a stronger barrier against liquefaction. Continuing the investigation into cases of soil liquefaction, The phenomena was seen to happen at a depth of 5 cm close to the surface (ru1). This phenomenon was noted in both unimproved and improved soils containing steel slag. The presence of steel slag did not have an impact on the liquefaction of the soil.

Furthermore, the times at which liquefaction occurred were very similar in all cases. The investigation also explored the potential for liquefaction at a 25 cm (ru2) depth. The liquefaction time it took for the soil to liquefy was the same for all cases of unreinforced soil and improved when steel slag was added, indicating that the slag did not affect the liquefaction time. Furthermore, the presence of steel slag was shown to not affect the liquefaction of sandy soil. In contrast to a depth of 5 cm, soil liquefaction for both (ru1) and (ru2) happens a few seconds early, at 25 cm below the surface. This implies that liquefaction occasionally reaches the top over the whole soil depth.

Table 3.
The period of time when the Halabjah earthquake caused the sandy soil to liquefy.

Situation involving soil	The liquefaction time (sec.) (ru1)	The liquefaction time (sec.) (ru2)
Unimproved soil	34.123	28.096
3% of steel slag	35.007	28.042
6% of steel slag	35.012	27.892
9% of steel slag	34.714	26.739
12% of steel slag	36.062	27.536
15% of steel slag	35.274	26.949

Edelweiss Applied Science and Technology
ISSN: 2576-8484
Vol. 8, No. 6: 9411-9424, 2024
DOI: 10.55214/25768484.v8i6.4018

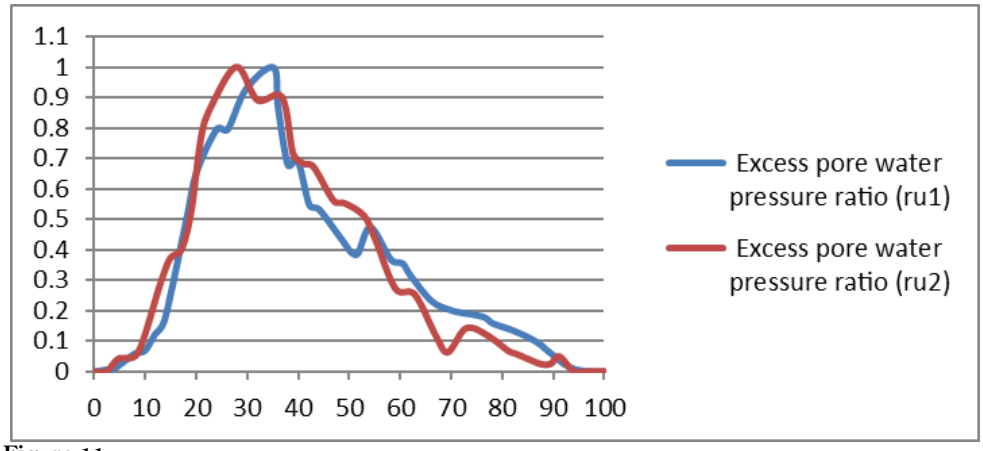

Figure 11.
Excess Pore water pressure ratio (ru) of unimproved saturated sandy soil at the Halabjah Earthquake.

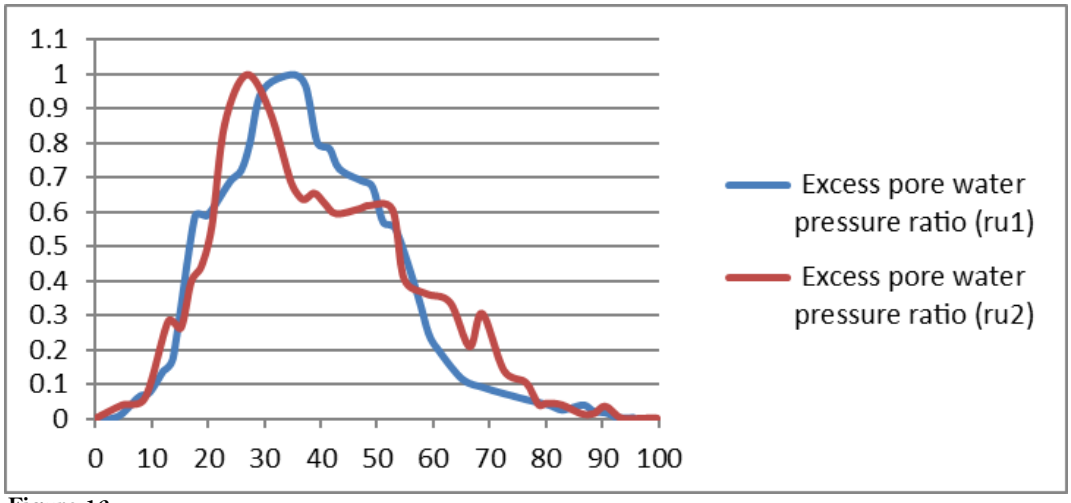

Figure 12.
Excess Pore water pressure ratio (ru) with 3% steel slag for saturated sandy soil at the Halabjah Earthquake.

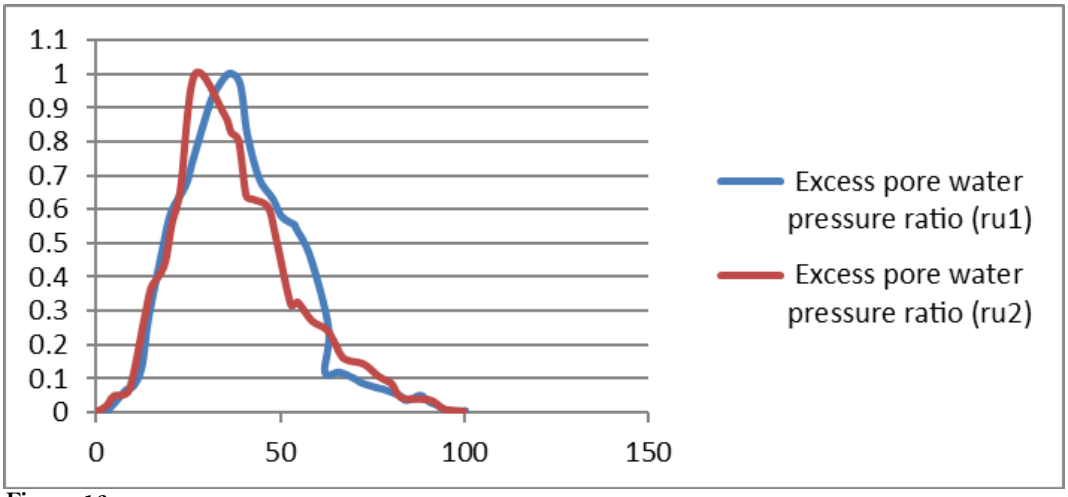

Figure 13.
Excess Pore water pressure ratio (ru) with 6% steel slag for saturated sandy soil at the Halabjah Earthquake.

Edelweiss Applied Science and Technology
ISSN: 2576-8484
Vol. 8, No. 6: 9411-9424, 2024
DOI: 10.55214/25768484.v8i6.4018

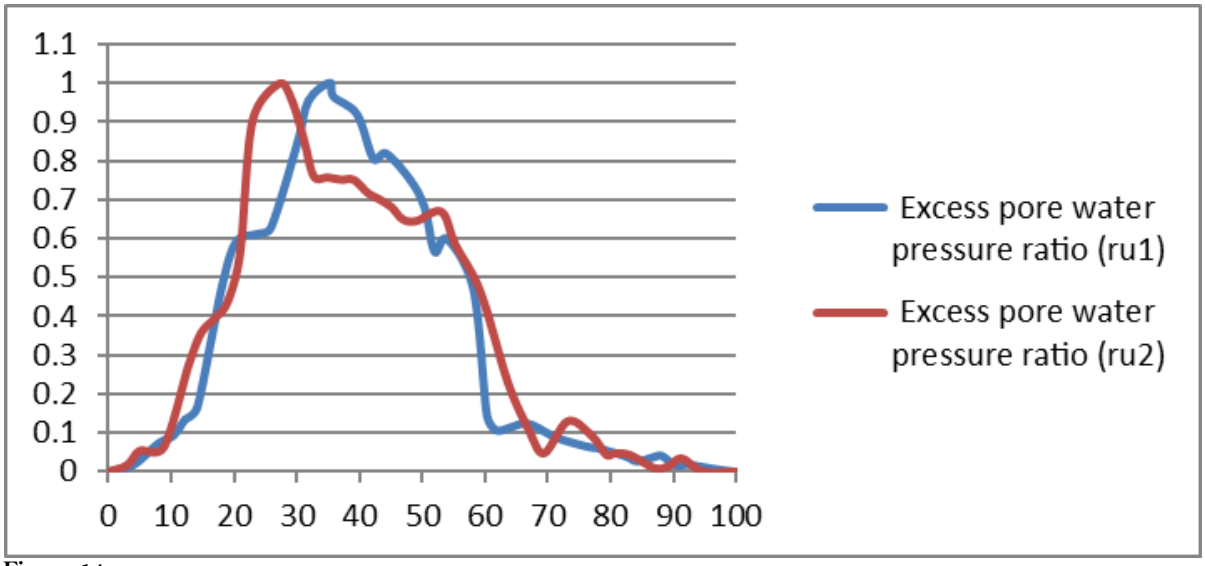

Figure 14.
Excess Pore water pressure ratio (ru) with 9% steel slag for saturated sandy soil at the Halabjah Earthquake.

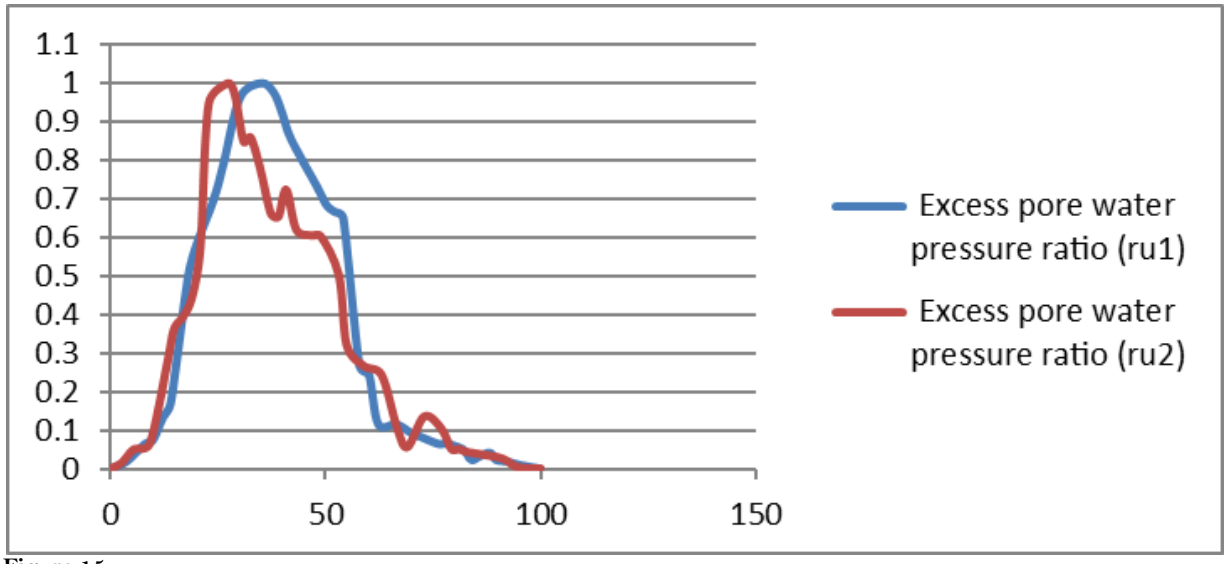

Figure 15.
Excess Pore water pressure ratio (ru) with 12% steel slag for saturated sandy soil at the Halabjah Earthquake.

Edelweiss Applied Science and Technology
ISSN: 2576-8484
Vol. 8, No. 6: 9411-9424, 2024
DOI: 10.55214/25768484.v8i6.4018

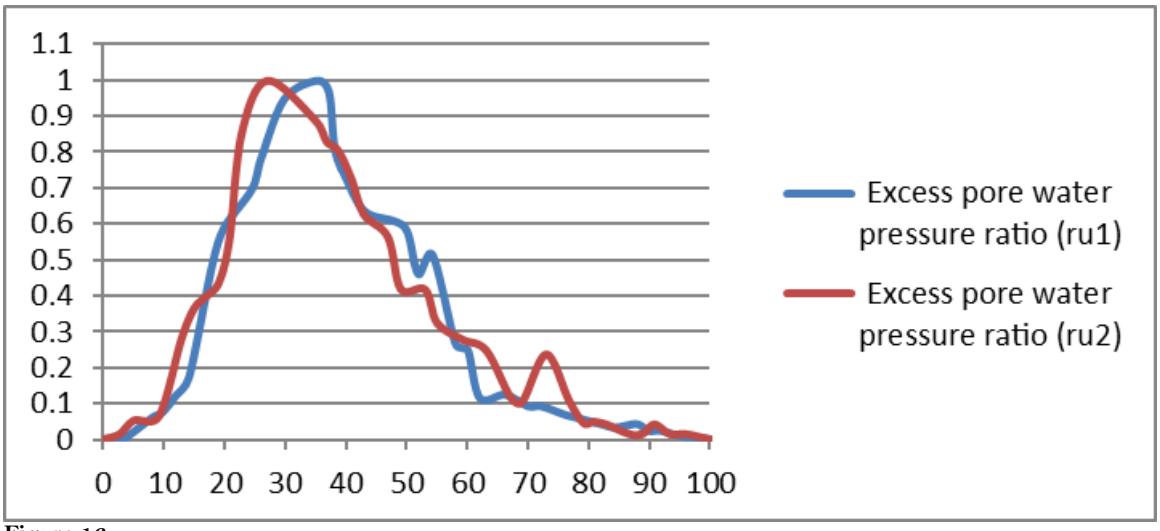

Figure 16.
Excess Pore water pressure ratio (ru) with 15% steel slag for saturated sandy soil at the Halabjah Earthquake.

4. Conclusion

Several shaking table tests were conducted to determine the maximum ground acceleration, duration of shaking, and depth of the sand model to investigate the surplus ratio of pore water pressure. The following important conclusions have been made:

1. An earthquake's strength increases in proportion to a liquefiable foundation's pore pressure ratio. The "rapid increase and slow dissipation" brought on by the quake increased the pore pressure within the foundation. There is a simultaneous phase of fast increases in pore pressure.
2. In contrast to the pore-pressure ratio at the foundation measuring point, the peak acceleration at a corresponding depth occurs later.
3. One significant aspect that can control how often sand liquefies as a result of variations in pore water pressure is the shaking duration of input motion. The sandy ground will liquefy multiple times during a shorter earthquake; this number will decrease with longer shaking.
4. It was found that when the amount of steel slag material increases, the pore water pressure at the surface, or at a depth of 5 cm called u1(pore water pressure), steadily drops.
5. It was also observed that, because the addition of steel slag had no effect on the time, the amount of time needed to attain the maximum value of pore water pressure was extremely similar to all other situations explored.

References

[1] Nepal, D. B., Deng, J., Chen, J., & Pokhrel, P. (2021). Factors influencing sand re-liquefaction in shaking table test. *Nepal J. Civil Eng*, *1*, 51-59.

[2] Lindh, P., & Lemenkova, P. (2022). Dynamics of strength gain in sandy soil stabilised with mixed binders evaluated by elastic P-waves during compressive loading. *Materials*, *15*(21), 7798.

[3] Bao, X., Jin, Z., Cui, H., Chen, X., & Xie, X. (2019). Soil liquefaction mitigation in geotechnical engineering: An overview of recently developed methods. *Soil Dynamics and Earthquake Engineering*, *120*, 273-291.

[4] Otsubo, M., Towhata, I., Hayashida, T., Liu, B., & Goto, S. (2016). Shaking table tests on liquefaction mitigation of embedded lifelines by backfilling with recycled materials. *Soils and Foundations*, *56*(3), 365-378.

[5] Hazarika, H., Pasha, S. M. K., Ishibashi, I., Yoshimoto, N., Kinoshita, T., Endo, S., ... & Hitosugi, T. (2020). Tire-chip reinforced foundation as liquefaction countermeasure for residential buildings. Soils and Foundations, 60(2), 315-326.

[6] Akinwumi, I. (2014). Soil modification by the application of steel slag. *Periodica Polytechnica Civil Engineering*, *58*(4), 371-377.
[7] Mominul, H. M., Alam, M. J., Ansary, M. A., & Karim, M. E. (2013). Dynamic properties and liquefaction potential of a sandy soil containing silt. In *Proceedings of the 18th international conference on soil mechanics and geotechnical engineering, Paris* (pp. 1539-1542).
[8] Bin Ye and Hailong Hu. Investigation on the reliquefaction behaviors of sand using shaking table tests. In GeoShanghai International Conference, pages 300–307. Springer, 2018.
[9] Hong, Y., Yang, Z., Orense, R. P., & Lu, Y. (2015, November). Investigation of sand-tire mixtures as liquefaction remedial measure. In Proceedings of the 10th Pacific conference on earthquake engineering, November, Sydney, Australia.
[10] Sağlam, S. (2011). Cyclic behavior of saturated low plastic fine soils.
[11] Chen GX, Chen S, Qi CZ, et al. Shaking table tests on a three-arch type subway station structure in a liquefiable soil. Bull Earthq Eng 2015;13(6):1675–701.
[12] Sun Haifeng. Study on earthquake damage mechanism of underground structures [D]. Doctor's degree thesis of institute of engineering mechanics. China Earthquake Administration; 2011 (In Chinese).
[13] Abed, N., & Abbas, J. K. (2020). Effect of iron filling on the behaviour of gypseous soils. *Journal of Mechanical Engineering Research and Developments*, *43*(7), 442-448.
[14] Hasen, N. A., & Abbas, J. K. (2024). Experimental Study of Shallow Foundation Settlement Under Dynamic Load In Reinforced Sandy Soil. *Proceedings on Engineering*, *6*(1), 171-178.

Edelweiss Applied Science and Technology
ISSN: 2576-8484
Vol. 8, No. 6: 9411-9424, 2024
DOI: 10.55214/25768484.v8i6.4018